PYRAMIDAL DEFECTS in GaN:Mg GROWN WITH Ga POLARITY

Z. Liliental-Weber, T. Tomaszewicz, D. Zakharov, and M.A. O'Keefe

Lawrence Berkeley National Laboratory, 1 Cyclotron Road, Berkeley, CA 94720 m/s 62/203

DISCLAIMER

This document was prepared as an account of work sponsored by the United States Government. While this document is believed to contain correct information, neither the United States Government nor any agency thereof, nor The Regents of the University of California, nor any of their employees, makes any warranty, express or implied, or assumes any legal responsibility for the accuracy, completeness, or usefulness of any information, apparatus, product, or process disclosed, or represents that its use would not infringe privately owned rights. Reference herein to any specific commercial product, process, or service by its trade name, trademark, manufacturer, or otherwise, does not necessarily constitute or imply its endorsement, recommendation, or favoring by the United States Government or any agency thereof, or The Regents of the University of California. The views and opinions of authors expressed herein do not necessarily state or reflect those of the United States Government or any agency thereof, or The Regents of the University of California.

Ernest Orlando Lawrence Berkeley National Laboratory is an equal opportunity employer.

Lawrence Berkeley National Laboratory -- LBNL-57521

PYRAMIDAL DEFECTS in GaN:Mg GROWN WITH Ga POLARITY

Z. Liliental-Weber, T. Tomaszewicz, D. Zakharov, and M.A. O'Keefe

Lawrence Berkeley National Laboratory, 1 Cyclotron Road, Berkeley, CA 94720 m/s 62/203

GaN can be easily grown with n-conductivity, but p-doping remains still difficult and not well understood. The only efficient p-type dopant is Mg, but the free hole concentration is limited to $2x10^{18}cm^{-3}$ for Mg concentrations in the low $10^{19}cm^{-3}$ range. This could limit further development of GaN based devices. Further increase of the Mg concentration, up to $1x10^{20}cm^{-3}$ leads to a decrease of the free hole concentration.

Transmission electron microscopy (TEM) studies show the formation of different types of Mg–rich defects [1,2]. The types of the defects strongly depend on crystal growth polarity. For bulk crystals grown with N-polarity, the planar defects are distributed at equal distances (20 unit cells of GaN). These defects were described as inversion domains [1]. For growth with Ga-polarity (for both bulk and MOCVD grown crystals) a different type of defects have been found [2]. These defects are three-dimensional Mg-rich hexagonal pyramids (or trapezoids) with their base on the (0001) plane and six walls formed on {11$\underline{2}$3} planes (schematic Fig. 1a). The defects appear in [11$\underline{2}$0] and [1$\underline{1}$00] cross-section TEM micrographs as triangular (Fig. 1b) and trapezoidal (Fig. 1c). The sides of these defects are inclined at 43° and 47° to the base depending on the above observation directions, respectively. The dimension of these pyramids varies depending on growth method (50Å-1000Å), but the angle between the base and their sides remain the same. The direction from the tip of the pyramid to its base (and from the shorter to the longer base for trapezoidal defects) is along the Ga to N matrix bond direction (Fig. 1a-d).

Our earlier studies using TEM and EDX show that these triangular and trapezoidal defects often have holes in their centers and are decorated by Mg on the defect walls [1]. We measured an expansion of the interplanar spacing along the c-axis on the defect base, consistent with Mg accumulation. Other researchers have observed similar types of defects and described them as inversion domain inclusions [3]. These two defects appear in the plan-view configuration as hexagons, and cannot be distinguished suggesting common origin of their formation.

In this studies pyramidal and trapezoidal defects were characterized using high-resolution electron microscopy (HRTEM) to obtain focal-series reconstruction of the electron exit-surface wave (ESW) leaving the specimen. Cowley & Iijima [4] showed that, without correction of spherical aberration by specialized hardware or focal-series reconstruction, imaging of the ESW phase is limited to the microscope resolution -- about 1.6Å for mid-voltage TEMs. However, ESW phase information is available out to the microscope information limit. This "extra" high-resolution information can be retrieved by focal-series reconstruction [5]. With appropriate measurements, one can distinguish between different elements contributing to the generated phase and, for mono-atomic columns, also define the number of atoms in the column. Since heavier atoms produce more phase change, in GaN the phase change produced by a Ga atom column is always stronger than the phase change produced by a N column with the equivalent number of atoms. With increasing numbers of atoms in the columns (increasing thickness), the phase change moves to produce a counterclockwise Argand-plane trajectory of the complex ESW vector at the atom position [6]. Since the change of phase for Ga is much faster than for N for the same number of atoms in the column, we can distinguish between Ga and N columns, determine crystal thickness and the crystal polarity.

Reconstructed exit wave phase from the area close to the pyramid tip showed blobs with two distinct intensity peaks, identified as due to Ga and N atomic columns. Using Argand plots, we confirmed that the phase of atoms described as Ga gave the highest peak, followed by a smaller phase peak described as N (Figs. 1 e-h). This identification of the atomic positions of Ga and N from the experimental reconstructed exit wave confirmed inversion of polarity within the pyramid compared to the matrix. In addition, it showed ab stacking in the matrix changes to bc stacking within the pyramid. This stacking arrangement holds through the entire pyramid and changes back to the ab stacking order above the pyramid base. Analysis of the reconstructed exit wave phase image from the pyramid side (Fig. 1e,f) indicates a shift of Ga atomic column positions from the matrix to the N position within the pyramid. In this way a 0.6Å±0.2Å displacement can be measured on the pyramid side between Ga positions in the matrix and within the pyramid [7].

References

1. Z. Liliental-Weber, et al, Phys. Rev. Letter. **82**, 2370 (1999).
2. Z. Liliental-Weber, et al, Phys. Rev. Lett. 93, 206102 (2004);
3. P. Vennegues, et al, Phys. Rev. Lett. 68, 235214 (2003);
4. J.M. Cowley and S. Iijima, Z. Naturforsch., **27a**, 445 (1972).
5. A. Thust, et al, Ultramicroscopy **64**, 211 (1996).
6. W. Sinkler and L. D. Marks Ultramicroscopy **75**, 251 (1999).
7. Supported by the Director, Office of Science, Office of Basic Energy Sciences, Materials Sciences and Engineering Division, DOE under contract DE-AC03-76SF00098.

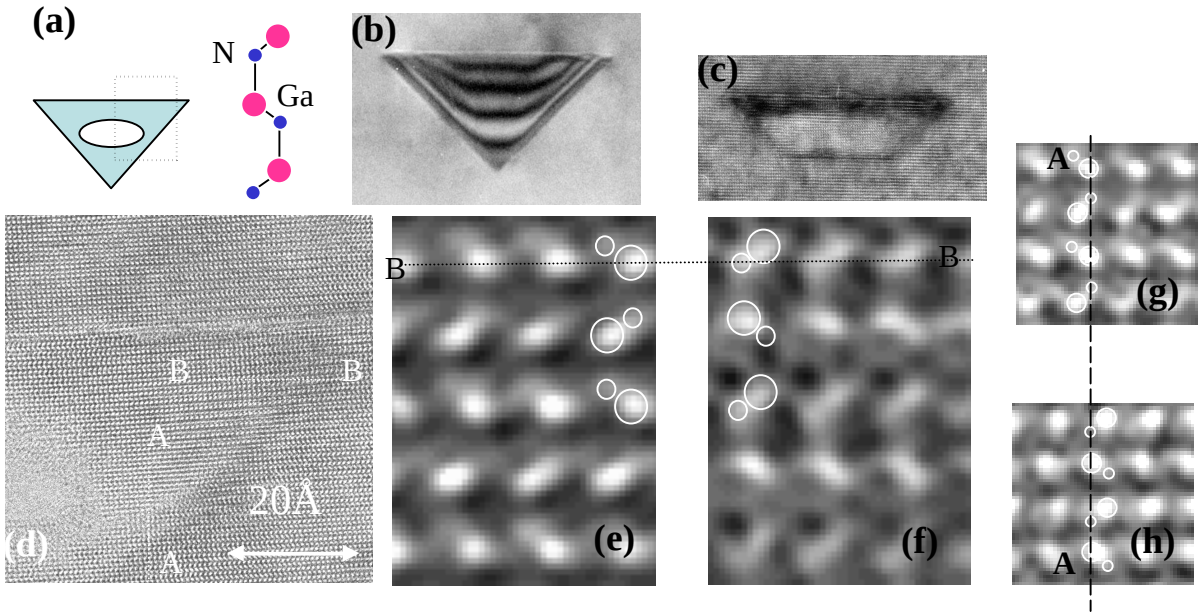

Fig. 1. (a) Schematic of pyramidal defect with outlined part shown in high resolution in (d). A hole formed inside the pyramid {proved experimentally in (d)} is also shown. Ga matrix polarity is indicated as well as arrangement of defects (b), (c) and (d) in this matrix; (b) and (c) Cross section of pyramidal and trapezoidal defects, respectively; (d) Cross-section image from the part of a pyramid {outlined in (a)}; (e) and (f) reconstructed exit wave phase from the side of the pyramid/matrix interface along the B-B line shown in (d): (e)-inside the pyramid, (f)-the matrix outside the pyramid, (g) and (h) reconstructed exit wave phase from the pyramid/matrix interface along the A-A line shown in (d); (e) inside the pyramid and (h) in the matrix below the pyramid aligned along c-axis.. Note stacking change within the defect (bc) compared to the matrix (ab).